IEEE Access
Multidisciplinary | Rapid Review | Open Access Journal

Received 31 July 2022, accepted 25 August 2022, date of publication 1 September 2022, date of current version 14 September 2022.

Digital Object Identifier 10.1109/ACCESS.2022.3203728

RESEARCH ARTICLE

An Improved C-DEEPSO Algorithm for Optimal Active-Reactive Power Dispatch in Microgrids With Electric Vehicles

CAROLINA GIL MARCELINO[1,2], GABRIEL MATOS CARDOSO LEITE[1,3], SILVIA JIMÉNEZ-FERNÁNDEZ[1], AND SANCHO SALCEDO-SANZ[1]

[1]Department of Signal Processing and Communications, Universidad de Alcalá (UAH), 28801 Alcalá de Henares, Spain
[2]Institute of Computing, Federal University of Rio de Janeiro (UFRJ), Rio de Janeiro 21941-901, Brazil
[3]Department of Systems and Computing, Federal University of Rio de Janeiro (UFRJ), Rio de Janeiro 21941-901, Brazil

Corresponding author: Carolina Gil Marcelino (carolina@ic.ufrj.br)

This work was supported in part by the European Union's Horizon 2020 Research and Innovation Program under the Marie Skłodowska-Curie under Grant 754382; in part by the Ministerio de Economía y Competitividad of Spain under Grant TIN2017-85887-C2-2-P; and in part by the Comunidad de Madrid, Programa Microrredes Inteligentes Comunidad de Madrid (PROMINT-CM) Project, under Grant P2018/EMT-4366. "The content of this publication does not reflect the official opinion of the European Union. Responsibility for the information and views expressed herein lies entirely with the author(s)."

ABSTRACT In the last years, our society's high energy demand has led to the proposal of novel ways of consuming and producing electricity. In this sense, many countries have encouraged micro generation, including the use of renewable sources such as solar irradiation and wind generation, or considering the insertion of electric vehicles as dispatchable units on the grid. This work addresses the Optimal active–reactive power dispatch (OARPD) problem (a type of optimal power flow (OPF) task) in microgrids considering electric vehicles. We used the modified IEEE 57 and IEEE 118 bus-systems test scenarios, in which thermoelectric generators were replaced by renewable generators. In particular, under the IEEE 118 bus system, electric vehicles were integrated into the grid. To solve the OARDP problem, we proposed the use and improvement of the Canonical Differential Evolutionary Particle Swarm Optimization (C-DEEPSO) algorithm. For further refinement in the search space, C-DEEPSO relies on local search operators. The results indicated that the proposed improved C-DEEPSO was able to show generation savings (in terms of millions of dollars) acting as a dispatch controller against two algorithms based on swarm intelligence.

INDEX TERMS Energy efficiency, optimal power flow, microgrids, swarm intelligence, C-DEEPSO.

I. INTRODUCTION

In recent years it has been understood that Renewable Energy Sources (RESs) will reduce ecological and financial issues in our technological societies. The concerns regarding environmental impacts associated with the constant increasing in fossil fuel use has led to a massive deployment of RESs, such as photovoltaic (PV) or wind-based (WT), and Energy Storage Systems (ESSs) in modern electrical power systems [1], [2]. However, an important problem that comes along with the RESs penetration in the grid is the uncertainty in forecasting wind speed and solar irradiation [3]. Moreover, with the presence of plug-in electric vehicles (PEVs), there is also the uncertainty related to consuming power from the grid (Grid to Vehicle (G2V)) and injecting power in the grid (Vehicle to Grid (V2G)) [4]. Hence, these uncertainties in the dynamics of the RESs must be taken into consideration to maintain a safe and profitable functioning of a power system.

The integration of RESs in smart grids provides not only benefits but also challenges related to the environment and countries' policies [5]. Among the numerous benefits of including both PV and WT generators in the grid, it is important to highlight the reduction in peak energy demand and consequently, a lessening in energy losses. However, these RESs rely on weather conditions, so this uncertainty may affect the reliability of the grid, and increase generation

The associate editor coordinating the review of this manuscript and approving it for publication was Giovanni Pau.

costs [6]. As an alternative to reduce voltage variations and power losses, energy storage services (ESS) are often employed [7]. Additionally, as the market absorption of electric vehicles (EVs) increases [8], PEVs play an important role in the grid. Unmanaged G2V may raise the load demand during peak hours leading to congestion of lines, therefore shortening the equipment's life due to the additional load burden and voltage fluctuations [9]. A possible alternative is to use management systems in EV charging stations.

A. RELATED WORK

According to Wu *et al.* [10], to maintain the system stability, charging stations must work in a coordinated way to meet the consumers' demand, while varying power balance within specified conditions. This can be done with either centralized or decentralized control. The decentralized control is also targeted in [11], in which the authors propose a stochastic model for the uncertain households' behaviour, EVs and distributed RESs, and bi-level stochastic programming to optimize the operation schedule under the proposed model. An attempt to control load demand through a price-responsive model for PEVs is presented in [12]. The proposed model is evaluated and tested in the IEEE 24-bus reliability test system, with results showing a reduction in the operation cost along with an increase in the security of the system. As an alternative to smart grids connected to the public grid that rely on thermal energy co-generators, Calise *et al.* [13] present a work that analyzes the integration of PEVs in G2V mode in such grids. The results showed that it was possible to detect an optimal strategy to charge the PEVs' fleet while minimizing the public grid power consumed.

Reversely to G2V operation, PEVs can also be used as ESSs to reduce intermittency in grid power in a V2G operation. A risk-averse strategy that attempts to optimize the profit of EV aggregators while providing a reasonable price for EV users is proposed in [14]. In this approach, a stochastic programming method is combined with an information gap decision theory (IGDT) model to take into account EV owners' behavior, charging electricity price, V2G degradation cost, and delivering PEVs with full SoC batteries at the time of departure under different scenarios. Another attempt to address both station owners and EV owners is presented in [15], with the co-existence of different types of charging stations in the grid, for instance, home charging (HCSs), battery swapping (BSSs), and public battery charging stations (BCSs). Then, the approach is analyzed in case studies using Australian electricity data.

A case study of a university campus in Pakistan with the presence of both PEVs and PV generators is used by Nasir *et al.* [16] to propose a linear programming-based energy management system that ensures power supply continuity. In [17], the authors propose a control approach for integrating PV generators and PEVs by allowing both to exchange electrical power. To address the problem of extreme weather events, Roudbari *et al.* [18] proposed a stochastic framework that takes into account both hourly reconfiguration of PEVs management and scheduling of resources considering the movement of PEVs' fleet and the weather effects.

In power systems, the optimal active-reactive power dispatch (OARPD) is a branch of optimal power flow (OPF) that aims at minimizing the operational cost of conventional generators while fulfilling constraints like nodal voltage limits, nodal balance power, and power flow equations, to name a few [19], [20]. OARPD involves complex nonlinear and non-convex minimization problems that, combined with the uncertainties of renewable energy sources, pose serious challenges in scheduling [21]. From the optimization point of view, besides being nonlinear and non-convex, OARPD problems also contain mixed integer and continuous design variables. These characteristics make such types of problems difficult to be solved using standard mathematical optimization techniques such as linear programming, non-linear programming or Newton's method [22], [23].

On the other hand, meta-heuristics methods do not come with the aforementioned disadvantages and have been widely applied to OPF problems [24]. Among the many meta-heuristics present in the literature, it is worth mentioning the Particle Swarm Optimization (PSO) [25], [26], Differential Evolution (DE) [27], [28] and Genetic Algorithm (GA) [29], [30]. In [31], the authors present a combination of a PSO-based algorithm and gravitational search algorithm (GSA) [32] that can achieve competitive results in a modification of the IEEE 30-bus test system to include two renewable energy sources, one WT and one PV. Another combination of a PSO-based algorithm, GSA, and Shannon Entropy is presented in [33]. This algorithm, named FPSOGSA, is applied to minimizing not only power losses but also voltage deviation regarding reactive power dispatch in both IEEE 30-Bus and IEEE 57-Bus test systems.

Similarly, Dabhi and Pandya [4] proposed HL_PS_VNSO, which is a combination of PSO and Levy Flight to compute step length with the Variable Neighborhood Search Optimization (VNS) algorithm to initialize the population near the optimal solution. The proposed algorithm achieved competitive performance when evaluated in a 25-bus microgrid network under 500 scenarios of uncertainty regarding RESs. Differential Evolution (DE) is also widely employed to solve OPF problems, as in [34], where an improved version of DE is proposed for reactive power management (RPM), in which the mutant vector is obtained from the average of three mutant vectors obtained by randomly selecting three best solutions from the current generation. The algorithm is then evaluated in IEEE 30-bus, 57-bus, 118-bus, and 300-bus test scenarios. However, the authors did not evaluate the inclusion of RESs in any of the test scenarios.

Wang *et al.* [35] proposed an adaptative genetic algorithm to improve resilience of microgrids with mobile energy storage systems to attackers. The solution presented relies on a three-level model that involves power surplus/shortage, power exchange and re-scheduling. In [36], a modified GA is employed in a AC OPF problem to ensure network's

minimal stability conditions, in which capacity and operational costs are included in a linearized version of the OPF problem.

Niu *et al.* [37] proposed a composite differential evolution algorithm that searches the parameters F and CR from an adaptative range of values (ARCoDE). ARCoDE obtained competitive results in a 41-bus wind power plant ORPD problem that contains 18 WTs. ORPD is a variation of OARPD that only targets reactive power. Another DE approach is presented in [38], where a step disturbance is employed to avoid local optima along with the CR decrease according to the number of iterations elapsed. Moreover, an adaption step is also employed to allow larger steps in the first iterations and smaller steps in the final iterations. The proposal is then evaluated in the IEEE 30-bus test system, targeting to minimize the expected security cost under six different scenarios, some including ESSs. A combination of DE operators and PSO algorithm, namely Canonical Differential Evolutionary Particle Swarm Optimization (C-DEEPSO), is employed to build an automatic electric dispatch controller for a 41-bus test system containing 18 wind generators under 96 different scenarios. Results showed that C-DEEPSO was able to reduce the daily losses by 6% [20].

B. CONTRIBUTIONS

In this paper, we tackle a problem of optimal active-reactive power dispatch in microgrids, considering renewable energy sources and electric vehicles. We propose the use of the C-DEEPSO approach in a problem over IEEE 57-bus test system, containing both WTs and PVs, and also in a larger system, the IEEE 118-bus test, containing WTs, PVs, and a fleet of PEVs. We propose a local search operator for PSO-based algorithms such as C-DEEPSO, which explores the neighbourhood of each particle by using not only the particle's velocity, but also fewer features than the original high dimensional space. Moreover, we also propose a new version of C-DEEPSO algorithm that uses the Cross-Entropy (CE) method for an initial deep search, which we dubbed CE-CDEEPSO. Therefore, the contributions of the present work are:

1) We propose an efficient way of solving active-reactive power dispatch problems in microgrids, considering renewable energy sources and electric vehicles.
2) We propose a novel combination of the Cross-Entropy (CE) [39] method with the C-DEEPSO algorithm, for an initial deep search mechanism, to find a promising basin of attraction to initialize C-DEEPSO's population.
3) We develop a local search mechanism that allows C-DEEPSO to explore the neighbourhood of each particle to find better solutions.
4) We analyze the robustness of the proposed algorithm in a scenario containing uncertainty from both PVs and WTs, and in a larger scenario that contains PVs, WTs, and also PEVs.
5) Finally, we use a statistical method entitled Connover Test with Holm-Bonferroni correction, for effective pairwise comparative studies.

The remainder of the paper is organized as follows: Section II provides the definitions of the addressed OARPD problem. Section III presents C-DEEPSO, along with CE and the proposed local search operator. Section IV contains the evaluations of the different test case scenarios and discussions of the results. Finally, Section V concludes the paper with some final remarks and future lines of research.

II. OPTIMAL POWER FLOW MODELING

In conventional OPF modeling, the Optimal Active-Reactive Power Dispatch Problem (OARPD) is addressed with the goal of minimizing the operational cost by means of total fuel cost [40], [41], [42], [43]. The associated objective function corresponds to a summation over quadratic equations of the scheduled power output of each generator. Equation (1) represents the total power production costs in ($/h)

$$\min\ C_{tot} = \sum_{i=1}^{N_G} \alpha_i + \beta_i \cdot Pg_i + \gamma_i \cdot Pg_i^2, \quad (\$/h), \tag{1}$$

in which C_{tot} is the total fuel cost of the system. The term P_{gi} is the power output of the i-th generator. N_G indicates the number of generators. The terms α, β, γ are the cost coefficients associated with each generator measured in ($/h), ($/MWh) and ($/MWh^2), respectively.

In this study, the OARPD benchmark used are the IEEE 57-Bus system and IEEE 118-Bus system, presented at the 2018 PES general meeting [44], which takes into account the stochastic behaviour of solar, wind and electric vehicles generation. To handle these new sources, three additional costs are added to Equation (1), which are the cost of wind power generators, solar photovoltaic generators and plug-in electric vehicles. Due to the stochasticity of the renewable energy generators, each cost must comprise factor for overestimated and underestimated condition [3]. An underestimated condition is defined as follows:

$$C_u = c_u(P_{a_i} - P_{s_i}) \tag{2}$$

$$\text{and } P_{a_i} > P_{s_i}. \tag{3}$$

Equation (2) specifies that, if the scheduled power from renewable generator i (P_{s_i}) is less than the power available at generator i (P_{a_i}), the difference $P_{a_i} - P_{s_i}$ of power that will not be used by the system is wasted. However, in real applications, this excess generation is directed to a energy storage system with a related cost given by c_u.

On the other hand, an overestimated condition is given by

$$C_o = c_o(P_{s_i} - P_{a_i}) \tag{4}$$

$$\text{and } P_{s_i} > P_{a_i}. \tag{5}$$

In an overestimated condition, the scheduled power from renewable generator i is higher than the total power available at generator i. In this situation, the lacking power given by Equation (4) must be requested from another renewable

(or not) energy source with a related cost c_o. Although the exact value of the available power at each renewable generator P_{a_i} is not available, a probability distribution of its value can be estimated using Monte Carlo [45]. Hence, it is possible to compute the overestimated and underestimated costs.

Based on the above definitions, the total cost of each each renewable energy generator can be calculated as:

$$C_{W_{tot}} = \sum_{i=1}^{N_W} C_{W_i}(W_{s_i}) + c_{o,W_i}(W_{s_i} - W_{a_i}) + c_{u,W_i}(W_{a_i} - W_{s_i}), \quad (6)$$

$$C_{PV_{tot}} = \sum_{i=1}^{N_{PV}} C_{PV_i}(PV_{s_i}) + c_{o,PV_i}(PV_{s_i} - PV_{a_i}) + c_{u,PV_i}(PV_{a_i} - PV_{s_i}), \quad (7)$$

$$C_{EV_{tot}} = \sum_{i=1}^{N_{EV}} C_{EV_i}(EV_{s_i}) + c_{o,EV_i}(EV_{s_i} - EV_{a_i}) + c_{u,EV_i}(EV_{a_i} - EV_{s_i}). \quad (8)$$

Then, Equation (1) can be modified to account for not only the total fuel cost but also the uncertainty costs of each renewable energy generator as follows:

$$\min\ C_{tot} = C_{W_{tot}} + C_{PV_{tot}} + C_{EV_{tot}} + \sum_{i=1}^{N_G} \alpha_i + \beta_i \cdot Pg_i + \gamma_i \cdot Pg_i^2, \quad (\$/h). \quad (9)$$

Furthermore, the problem must also satisfy the following constraints:

$$P_i = Pg_i - Pl_i = \sum_{j=1}^{NB} U_i U_j \begin{bmatrix} G_{ij}\cos(\delta_i - \delta_j) + \\ B_{ij}\sin(\delta_i - \delta_j) \end{bmatrix}, \quad (10)$$

$$\forall_i \in NB, \forall_s \in NS; \quad (11)$$

$$Q_i = Qg_i - Ql_i = \sum_{j=1}^{NB} U_i U_j \begin{bmatrix} G_{ij}\sin(\delta_i - \delta_j) + \\ B_{ij}\cos(\delta_i - \delta_j) \end{bmatrix}, \quad (12)$$

$$\forall_i \in NB, \forall_s \in NS; \quad (13)$$

$$\underline{U_i} \leqslant U_i \leqslant \overline{U_i}, \forall_i \in NB, \forall_s \in NS; \quad (14)$$

$$\left|S_{ij}\right| \leqslant \overline{S_{ij}}, \forall_i \in NC, \forall_s \in NS; \quad (15)$$

$$\left|S_{ji}\right| \leqslant \overline{S_{ij}}, \forall_i \in NC, \forall_s \in NS; \quad (16)$$

$$\underline{Pg_i} \leqslant Pg_i \leqslant \overline{P_i}, \forall_i \in NG, \forall_s \in NS; \quad (17)$$

$$\underline{Qg_i} \leqslant Qg_i \leqslant \overline{Q_i}, \forall_i \in NG, \forall_s \in NS; \quad (18)$$

$$\underline{t_i} \leqslant t_i \leqslant \overline{t_i}, \forall_i \in NOLTC, t_i \in \forall_s \in NS; \quad (19)$$

$$0 \leqslant q_i \leqslant 1, \forall_i \in NSHUNT, q_i \in Z, \forall_s \in NS. \quad (20)$$

Table 1 presents an explanation of the meaning of each quantity variable in the constraints given by Equation (10).

TABLE 1. Constraint variables.

Symbol	Quantity	Unit
P_i	Active power injected	MW
Q_i	Reactive power	MVar
Pl	Active power load	MW
U_i	Voltage magnitude	kV
δ_i	Voltage angle	radians
S_{ij}	Apparent power flow injection at the sending end of transmission connecting bus i to bus j	MVA
S_{ji}	Apparent power flow injection at the receiving end of transmission connecting bus i to bus j	MVA
P_{g_i}	Active power generation	MW
Q_{g_i}	Reactive power generation	MVar
t_i	Tap setting position of the On-Load Tap Changer (OLTC)	-
q_i	State of the capacitor/reactor bank	-
NG	Number of generators	-
NB	Number of buses	-
NC	Number of circuits in the network	-
$NOLTC$	Number of OLTC transformers	-
$NSHUNT$	Number of capacitor/reactor banks	-
NS	Number of scenarios for the expected operation scenario	-

III. IMPROVED C-DEEPSO WITH LOCAL SEACH APROACHES

Particle Swarm Optimization (PSO) is an evolutionary-type algorithm (EA) inspired by the swarm intelligence phenomena, firstly proposed in [46]. In the PSO, the new velocity of an individual particle is updated towards the directions of the past velocity, the particle's best position ever found and the best position found by the swarm. Thus, the new particle's position is obtained by adding the new velocity to its current position. Canonical Differential Evolutionary Particle Swarm Optimization (C-DEEPSO) proposed in [41] is a different approach based on PSO foundations, that merges both PSO and Differential Evolution (DE) concepts. In C-DEEPSO, a particle is controlled by a movement rule that is calculated according to Equation (21):

$$\begin{cases} V_t = w_I^* \times V_{t-1} + w_A^* \times (X_{st} + F(X_r - X_{t-1})) \\ \qquad + w_C^* \times C \times (X_{gb}^* - X_{t-1}), \\ X_t = X_{t-1} + V_t, \end{cases} \quad (21)$$

where X_{st} is a different individual from X_{t-1} obtained from DE operator. Unlike classic PSO, that uses only each particle's best position, C-DEEPSO uses not only particle's best position, but also a collective memory of solutions, to provide a wider view of the search space for each individual. In this work we chose to generate X_{st} according to *rand/1/bin* DE strategy.

In Equation (21), the subscript t indicates the current generation, X is the current solution or particle's position, V denotes the velocity of the particle and X_{gb} is the best solution ever found by the swarm. Moreover, the term C represents a $n \times n$ diagonal matrix of Bernoulli random variables that are sampled for each particle. The probability used to generate the matrix C is a parameter denoted communication probability, P. The intuition behind using matrix C is based on a technique named "stochastic star communication topology" [47]. This technique restricts the amount of information that can be used from the global best at each iteration. After a generation, C-DEEPSO saves a small subset of the best solutions in the swarm in a memory called *Memory B* [48]. Hence, with this

memory mechanism, the term X_r is obtained according to the following strategies:

1) $S_g - rnd$: sampled as a uniform recombination from particles of the current generation;
2) $P_b - rnd$: sampled as a uniform recombination from particles in *Memory B*, and
3) $S_gP_b - rnd$: sampled as a uniform recombination from the union of both particles in the current generation and particles in *Memory B*, which is a combination of $S_g - rnd$ and $P_b - rnd$.

Furthermore, the inertia, assimilation and communication weights are mutated according to the rule

$$w^* = w + \tau \times N(0, 1), \tag{22}$$

where τ is the mutation rate controlled by the user. This rule adds a standard Gaussian noise scaled by τ to weights. It is important to note that the mutation must guarantee weights to be within [0, 1] interval. Besides, to avoid getting trapped in a particular region of the search space, X_{gb} is also mutated in Equation 21. Similarly to the mutation in the weights, the mutation in X_{gb} is obtained by Equation (23),

$$X^*_{gb} = X_{gb}[1 + \tau \times N(0, 1)]. \tag{23}$$

A. INITIAL DEEP SEARCH USING CROSS-ENTROPY METHOD

The Cross-Entropy (CE) method was proposed by [39] for estimating probabilities of rare events in complex stochastic networks. CE is a Monte-Carlo technique for sampling and optimization that can be applied to combinatorial and continuous problems. According to [49] the CE method is composed by a iterative procedure having each step divided into two main moves:

- Generate a random data sample (trajectories, vectors, etc.) according to a specified mechanism;
- Update the parameters of the random mechanism based on the data to produce a ''better'' sample in the next iteration.

The basic idea for using CE in complex optimization tasks is to interpret them as rare event estimation problems. From this, Carvalho *et al.* [50] proposed a version to solve continuous problems and applied it to solve a OARDP problem. The implemented code is available on [44] sources. Here, we use the CE method as an initial deep search operator for the C-DEEPSO algorithm.

B. SWARM MEMORY VELOCITY WITH LOCAL SEARCH MECHANISM

When dealing with real-world optimization problems, algorithms have to be carefully designed to handle difficulties, such as the presence of several local minima in the search space or a high number of optimization variables, among others. Based on such difficulties, we propose a local search mechanism that explores the awareness of the each particle, prior to moving to the next position. In this awareness mechanism, particles look in other three directions besides the new

Algorithm 1 CE Method for Initial Deep Search

Require: $\boldsymbol{\mu}_0$, Σ_0, N, α, β and rarity parameter ρ
  $k \leftarrow 0$
  while $\max(\Sigma_k) < \epsilon$ **do**
    $k \leftarrow k + 1$
    Sample $X_1, \ldots, X_N \sim \mathcal{N}(\boldsymbol{\mu}_{k-1}, \Sigma_{k-1})$
    Compute $P \leftarrow \{S(X_1), \ldots, S(X_N)\}$
    Sort P in ascending order
    $\gamma \leftarrow \rho$th quantile of P
    $N_{elite} \leftarrow \rho N$; $\psi \leftarrow \{\}$
    for $S(X_i) \in P$ **do**
      if $S(X_i) < \gamma \wedge |\psi| < N_{elite}$ **then**
        $\psi \leftarrow \psi \cup \{X_i\}$
      else
        break
      end if
    end for
    $\boldsymbol{\mu_k} \leftarrow \frac{1}{N_{elite}} \sum_{i \in \psi} X_i$
    $\Sigma_k \leftarrow \frac{1}{N_{elite}-1} \sum_{i \in \psi} (X_i - \boldsymbol{\mu_k})^2$
    $\boldsymbol{\mu_k} \leftarrow \alpha \boldsymbol{\mu_k} + (1 - \alpha)\boldsymbol{\mu_{k-1}}$
    $\Sigma_k \leftarrow \alpha \Sigma_k + (1 - \alpha)\Sigma_{k-1}$
  end while
  return $X_1, \ldots, X_N$

V_t. These new directions are dubbed V_{south}, V_{east} and V_{west}. The V_{south} direction is obtained by inverting the direction of V_t. The V_{east} direction is calculated as a random vector with X_{t-1} as origin, that lies in a randomly generated plane perpendicular to V_t passing through X_{t-1}.

This plane is generated by choosing at random $d \leq D - 1$ features from the original $D-$dimensional space. Similarly to V_{south} direction, V_{west} direction is generated by inverting the vector V_{east}. Figure 1 illustrates the local search mechanism. Then, four new positions for the particle are evaluated: X_{south}, X_{east}, X_{west} and the position obtained by following V_t, namely X_{V_t}. The position and velocity that lead to the best fitness are assigned to X_t and V_t, respectively. This mechanism helps particles to search in the whereabouts of their current position in the search space for better movements than the one calculated by the movement rule. By choosing a small d, each particle can search for a better movement in fewer dimensions than the original decision space. However, since this local search mechanism requires four times more function evaluations, it can only be applied a predefined number of times and at random iterations. The Algorithm 2 shows the local search mechanism. As a result, Algorithm 3 presents the proposed algorithm combining both Cross-Entropy Method and proposed local search operator.

IV. EXPERIMENTAL DESIGN AND RESULTS

In this work we are measuring the performance of the population based algorithms named PSO, CE-EPSO [50] and the improved C-DEEPSO (applying local search operator's – the CE-CDEESPO) proposed here to solve the OARDP

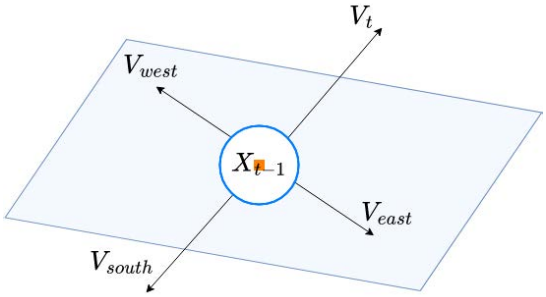

FIGURE 1. Illustration of the three search directions generated by the local search mechanism for one particle.

Algorithm 2 Local Search Mechanism

Require: $X_{t-1}, X_{lb}, X_{ub}, d$
  Compute velocity V_t
  $V_{south} \leftarrow -1 \cdot V_t$
  $X_{plane} \leftarrow \{0\}^D$
  Sample $y_1, \ldots, y_d, y_{d+1} \sim \mathcal{U}(1, D)$
  for $i \in (1, d)$ **do**
    $X_{plane}[y_i] \leftarrow \mathcal{U}(X_{lb}[y_i], X_{ub}[y_i])$
  end for
  $X_{rand} \leftarrow (X_{rand} - X_{t-1}) \odot V_t$
  if $V_t[y_{d+1}] > 0$ **then**
    $X_{plane}[y_{d+1}] \leftarrow X_{t-1}[y_{d+1}] - 1/V_t[y_{d+1}] \times \sum_{y_i \neq y_{d+1}} X_{plane}[y_i]$
  else
    $X_{plane}[y_{d+1}] \leftarrow X_{t-1}[y_{d+1}] - \sum_{y_i \neq y_{d+1}} X_{plane}[y_i]$
  end if
  $V_t \leftarrow argmin_{V \in \{V_t, V_{south}, V_{east}, V_{west}\}} f(X_{t-1} + V)$
  $X_t \leftarrow X_{t-1} + V_t$

problem in the IEEE 57 and 118 Bus-Systems, with renewable generators aggregated. The population size was defined as 100 particles for all algorithms. As initialization parameters of the CE-EPSO and CE-CDEEPSO algorithms, we have empirically defined a weight mutation rate equal to 70%, and a communication rate equal to 20%. PSO used as parameters: 0.9 for inertia weight and 2.0 for both cognitive and social coefficients. For all algorithms, the rates used in the local search phase performed by the cross-entropy method have been sigma equal to 80%.

Specifically for Cross-Entropy, we used 1.5×10^4 fitness evaluations to perform the CE local search procedure. The number of local search operator calls (swarm memory velocity) is 20. The stopping criterion defined for all algorithms in IEEE 57 Bus systems was 3×10^4 fitness evaluations (FEs). For the IEEE 118-Bus systems the stop criterion was 9×10^4 power flows fitness evaluations (FEs), where that in every time it is calculate 6 (time instances) power flows for each set of decision variables. We perform the computational simulation using an Intel(R) Core(TM) i9-10900X CPU@3.70GHz and 64 GB RAM, with Windows 10 Pro.

Algorithm 3 Improved C-DEEPSO With Local Search Operators

Require: population size (NP), mutation rate τ, communication rate (P), memory size (MB), dimension (D), dimension (d), number of local search operator calls (n_ls), number of CE calls (N_{CE}), lower bounds (X_{lb}) and upper bounds (X_{ub})
  Set the generation number $t = 0$
  Initialize the NP individuals in the population at random according to $\mathcal{U}(X_{lb}, X_{ub})$
  Evaluate the current population
  Update the global best X_{gb}
  Sample n_ls generation numbers to apply local search operator and store in N_{ls}
  while *stopping criterion is not satisfied* **do**
    if $t < N_{CE}$ **then**
      Run CE
    else
      for individual i in the population NP **do**
        Calculate X_r using the strategy $S_g P_B - rnd$
        Copy current individual X_{t-1}
        Mutate strategy parameters w_I, w_A, w_C and X^*_{gb}
        Apply movement rule in current individual X_{t-1}
        if $t \in N_{ls}$ **then**
          $V_t \leftarrow LocalSearch(X_{t-1}, X_{lb}, X_{ub}, d)$
        end if
        Evaluate current individual X_t and its copy
        Select the fittest individual to proceed to next generation
        Update personal best individual
      end for
      Update memory MB
      $t = t + 1$
    end if
  end while

The evolutionary meta-heuristics' code is implemented in Matlab R2020b.

A. PRELIMINARY EXPERIMENT

A preliminary experiment is run using two benchmark functions from literature, Rastringin and Rosenbrock. The rationale behind this experiment is to verify the results obtained by the CE-CDEEPSO with local search, compared to CE-EPSO with local search and results by standard PSO, with and without local search procedure. The initialization parameters for both CE-EPSO and CE-CDEEPSO are the following: Mutation rate 0.6 and Communication rate 0.2. The number of total fitness values was set as 5×10^5. For each dimension (30, 50, 100), the algorithm are tested using the population size of 60 and 10 independent runs. Equations (24) and (25) show the benchmark functions:

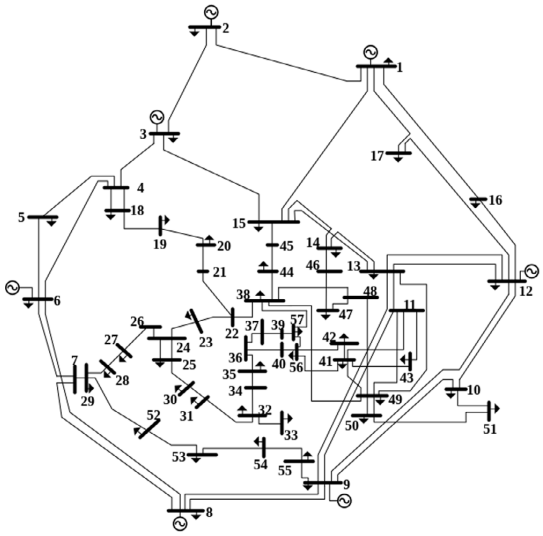

FIGURE 2. Diagram of IEEE 57 bus system.

- Rastringin function - Multimodal - Goal = 0,

$$f(x) = \sum_{i=1}^{D} [x_i^2 - 10\cos(2\pi x_i) + 10]. \quad (24)$$

- Rosenbrock function - Unimodal - Goal = 0,

$$f(x) = \sum_{i=1}^{D-1} [100(x_i^2 - x_{i+1})^2 + (x_i - 1)^2]. \quad (25)$$

Table 2 shows the results of the PSO, CE-EPSO and CE-CDEEPSO algorithms. The results indicated that CE-CDEEPSO obtained a competitive performance compared to both standard PSO and CE-EPSO algorithms in solving Rastringin and Rosenbrock functions with different dimensions. Furthermore, regarding standard PSO performance, the proposed local search mechanism was able to significantly improve the results. Hence, CE-CDEEPSO is able to outperform the results obtained by the base algorithms in benchmark functions.

B. STATIC OPF PROBLEM IN A MICROGRID

We choose simulate in a first moment the IEEE 57 Bus-System (see Figure 2)). To use the mathematical modeling described in Section II. In this case, for the IEEE 57 only equations (6) and (7) are considered as an additional cost for generation via solar panels and wind turbines. Two test scenarios were considered: (1) Replacing three thermoelectric generators with wind generators, and; (2) Replacing three thermoelectric generators with wind and solar generators.

The IEEE 57 Bus-system presented in Figure (2) is composed by 7 generators, 42 loads, 63 lines, 16 stepwise transformers, 2 fixed tap transformers, and 3 shunt compensation. Usually, the goal in the ORAPD is to minimize the total fuel cost while fulfilling constraints (nodal balance of power, nodal voltages, allowable branch power flows, generator reactive power capability, and maximum active power output of slack generator) for normal (non-contingency) and selected N-1 conditions. In this work, the goal is to minimize the total fuel cost of the traditional generators plus the expected uncertainty cost for renewable energy generators (as explained in Section II). We conduct a experimental design to verify the efficiency of some evolutionary meta-heuristics when solving the OARPD problem. The simulation follows the characteristics:

- Optimization variables: 35 variables, comprising 13 continuous variables related to generator's active power outputs (6, the slack is not considered here, since the injected power is given by the power flow) and generator's bus voltage set-points (7), 15 discrete variables related to stepwise adjustable on-load transformers' tap positions, 3 binary variables related to switchable shunt compensation devices, and 4 controllable loads, and;
- Considered contingencies (N-1 conditions): outages at branches 8 and 50.

The first experiment consists of validating the performance of each algorithm by solving the OARPD problem in which generators 2, 6, and 9 have been replaced by wind generators. In this case, PSO, CE-EPSO and CE-CDEEPSO were executed a total of 12 times. Figure (3) shows the mean convergence line obtained by each algorithm. Visually, it is possible to notice that the standard PSO algorithm converges faster in relation to others. CE-CDEEPSO shows a consistent decline before 5000 function evaluations. Moreover, we can see that C-DEEPSO obtains the smallest average fitness function value over 12 runs outperforming PSO and CE-EPSO. However, a better way to evaluate the results obtained is through the analysis of some performance measure.

A non-parametric test can be performed and in this work we analyzed the Boxplot behaviour. Boxplots are not only useful to analyze the range and distribution of the data, but sometimes it can provide information about the true difference among the means. If the notches in the boxplots do not overlap, it can be concluded, with 95% confidence, that the true means do differ [51]. Figure (4) shows the boxplot graphs. Since the boxplots presented do not show overlap, we can conclude that there are differences among the true means of algorithms.

As visualized by Figure (3), CE-CDEEPSO generates savings of \$14312.12/h when compared to CE-EPSO. In a monthly projection, this economy reaches in average ten million dollars. As a solution to be applied to the system, we chose the median result of 12 runs. Table 3[1] represents the median optimized solution for the IEEE Bus System with Wind generators.

The same test case (IEEE 57 Bus-System) was used for the second experiment in static optimization. the change made include a solar generator in place of one wind turbine. Figure (5) shows the average line of convergence of 12 runs of each algorithm. We can see that around 10000 fitness

[1]Legend: Generator's active power outputs (G_{apo}); Generator's bus voltage set-points ($Gbvsp$); Tap positions (T_p); Shunt compensation devices (S_{cd}).

TABLE 2. Summary of the obtained results on each benchmark function.

		Rastringin		Rosenbrock	
Dimension	Algorithm	Mean	Std	Mean	Std
30	PSO	161.86	19.74	1528.38	567.20
	PSO w/ Local Search	0.32	0.68	28.95	0.17
	CE-EPSO w/ Local Search	0.00	0.00	25.26	0.32
	CE-CDEEPSO w/ Local Search	0.00	0.00	22.65	0.75
50	PSO	332.02	26.65	5479.05	1731.33
	PSO w/ Local Search	1.11	0.88	48.96	0.26
	CE-EPSO w/ Local Search	0.00	0.00	45.65	0.66
	CE-CDEEPSO w/ Local Search	0.00	0.00	43.48	0.79
100	PSO	824.74	58.57	17446.13	5763.48
	PSO w/ Local Search	2.31	3.12	98.99	0.12
	CE-EPSO w/ Local Search	0.00	0.00	96.63	1.16
	CE-CDEEPSO w/ Local Search	0.00	0.00	94.85	1.31

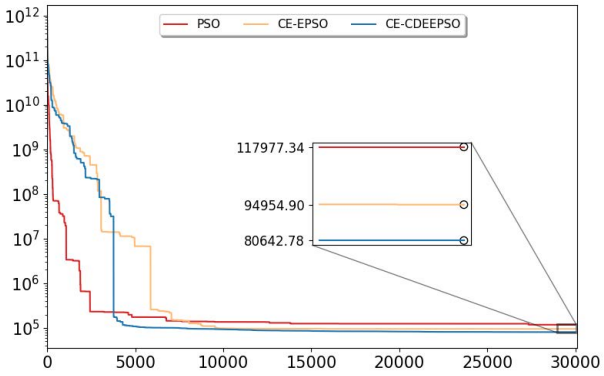

FIGURE 3. Convergence line of the IEEE 57 bus system with wind generators.

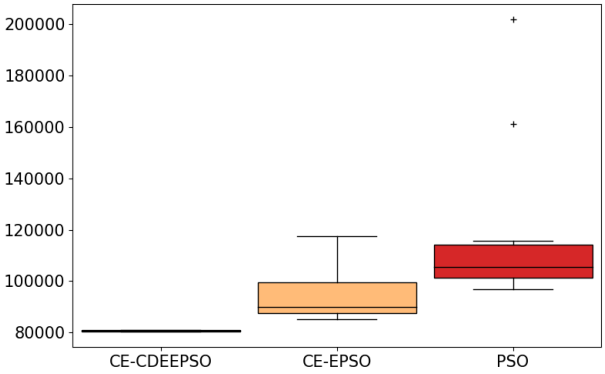

FIGURE 4. Boxplot results of the IEEE 57 bus system with wind generators.

TABLE 3. IEEE 57 bus-system: optimized results of the median solution: grid with Wind generators.

IEEE 57	Bus-System with Wind generators		
Variables	CE-DEEPSO	CE+EPSO	PSO
G_{apo}	128.40	133.05	121.79
G_{apo}	42.18	46.33	119.72
G_{apo}	135.28	130.14	121.78
G_{apo}	251.91	275.44	485.95
G_{apo}	128.35	133.45	141.90
G_{apo}	250.89	228.53	343.91
$Gbvsp$	1.03	1.03	1.04
$Gbvsp$	1.02	1.03	1.03
$Gbvsp$	1.02	1.02	1.04
$Gbvsp$	1.03	1.04	1.04
$Gbvsp$	1.04	1.05	1.04
$Gbvsp$	1.01	1.01	1.02
$Gbvsp$	1.02	1.01	1.03
T_p	-5	-6	9
T_p	-4	-2	6
T_p	-5	3	-6
T_p	1	-1	8
T_p	-1	-2	-8
T_p	-7	-3	2
T_p	-6	-5	0
T_p	0	1	1
T_p	-3	-3	-1
T_p	-6	2	0
T_p	1	-3	-7
T_p	-5	1	-2
T_p	0	0	-3
T_p	0	6	-1
T_p	5	-5	0
T_p	0	0	1
T_p	1	1	1
T_p	0	1	1
S_{cd}	110.55	50.75	154.25
S_{cd}	191.11	300.00	415.03
S_{cd}	10.63	10.75	40.12
S_{cd}	11.27	10.40	47.36

function evaluations, the algorithms begin to stabilize their convergences. The standard PSO algorithm clearly has a very high average value. We can see that when replacing a wind generator with solar generation sources, the cost of the operation decreases. The convergences of CE-CDEEPSO and CE-EPSO visually appear to be close. When performing an enlargement of the graph, we see that on average CE-CDEEPSO outperforms CE-EPSO.

The average behavior of the results remains as seen in the system only with the replacement of thermometric generators by wind turbines. Through the analysis of the boxplots presented in Figure (6), we can see that with 95% confidence, that the true algorithms means results do differ. Therefore, we can say that CE-CDEEPSO has lower average results than those presented by CE-EPSO. Our algorithm CE-CDEEPSO was able to save $4484.20/h. Following it, in a monthly projection CE-CDEEPSO saves an average of

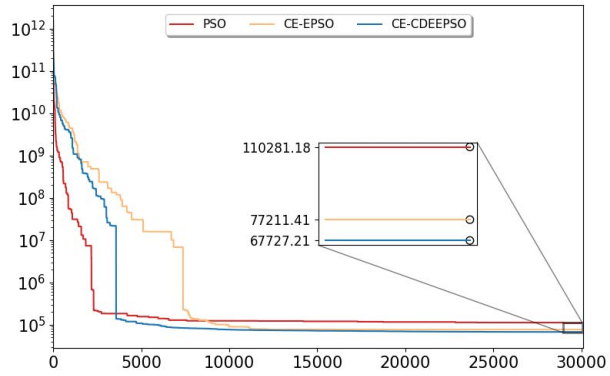

FIGURE 5. Diagram of the IEEE 57 bus system with wind/solar generators.

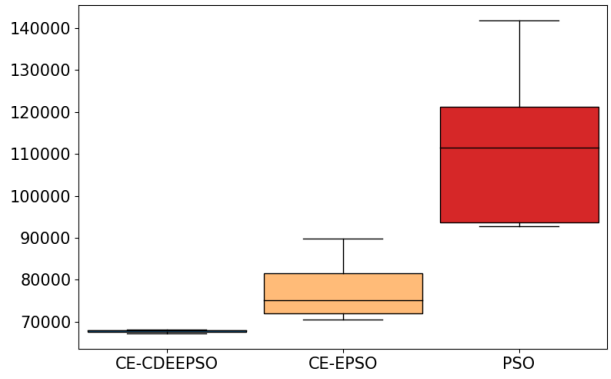

FIGURE 6. Diagram of the IEEE 57 bus system with wind/solar generators.

3.2 million dollars. Table 4 presents the median solution of each algorithm to be applied to the problem.

C. DYNAMIC OPF PROBLEM IN MICROGRIDS INCLUDING ELECTRIC VEHICLES

The dynamic OPF approach has been adopted in 2018 by IEEE PES using as test scenario the IEEE 118 Bus-System. The test case includes two wind turbine-generator and two solar photovoltaic (PV) systems replacing thermoelectric generators in the grid. Additionally, four electric vehicles are considered, and the problems are evaluated over six time instances (so, the number of decision variables and constraints will be multiplied by six). Thus, this problem is recognized as a Dynamic OPF [38], in which a solution comprises the power flow for each of the time instances.

Figure (7) represents the unifilar diagram of IEEE 118 Bus-System in witch the grid is composed by 54 generators, 99 loads, 177 lines/cables, 9 stepwise transformers, and 14 shunt compensation. The system addressed here considers security constraints to the normal (non-contingency) and selected N-1 conditions. In this work, the goal is to minimize the total fuel cost of the traditional generators plus the expected uncertainty cost for renewable energy generators (as explained in Section (II). We conduct a experimental design to verify the efficiency of some evolutionary meta-heuristics

TABLE 4. IEEE 57 bus-system: optimized results of the median solution: grid with wind/solar generators.

IEEE 57	Bus-System with Wind/Solar generators		
Variables	CE-DEEPSO	CE+EPSO	PSO
G_{apo}	131.23	132.39	128.87
G_{apo}	53.00	42.00	130.21
G_{apo}	45.99	46.38	65.38
G_{apo}	290.60	323.19	460.02
G_{apo}	141.31	136.30	144.21
G_{apo}	244.94	255.43	345.69
$Gbvsp$	1.05	0.97	1.04
$Gbvsp$	1.04	0.98	1.03
$Gbvsp$	1.02	0.98	1.04
$Gbvsp$	1.04	0.98	1.05
$Gbvsp$	1.05	0.98	1.05
$Gbvsp$	1.02	0.96	1.03
$Gbvsp$	1.03	0.97	1.04
T_p	4.00	-1.00	9.00
T_p	1.00	-4.00	-4.00
T_p	4.00	1.00	-2.00
T_p	0.00	-2.00	9.00
T_p	2.00	-10.00	2.00
T_p	-3.00	-5.00	-1.00
T_p	-6.00	-10.00	5.00
T_p	-6.00	-7.00	-8.00
T_p	-10.00	-8.00	-1.00
T_p	-1.00	-7.00	-1.00
T_p	-8.00	-9.00	-2.00
T_p	-6.00	-10.00	-6.00
T_p	8.00	-2.00	-1.00
T_p	2.00	-5.00	-1.00
T_p	0.00	-9.00	9.00
T_p	0.00	1.00	1.00
T_p	1.00	1.00	1.00
T_p	0.00	1.00	1.00
S_{cd}	58.22	50.00	141.01
S_{cd}	196.01	300.00	418.42
S_{cd}	23.69	9.90	43.52
S_{cd}	10.62	9.91	45.40

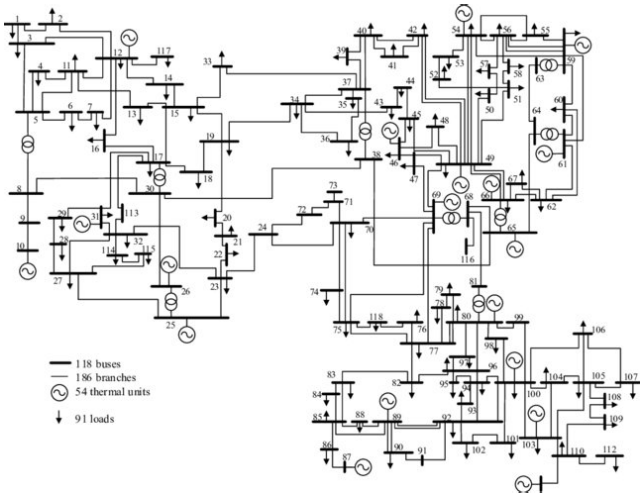

FIGURE 7. Diagram of IEEE 118 bus system.

when solving the OARPD problem. The simulation follows the characteristics:

- Optimization variables: 6 x 130 variables, comprising 107 continuous variables describing generator active power outputs (53, the slack is not considered here, since

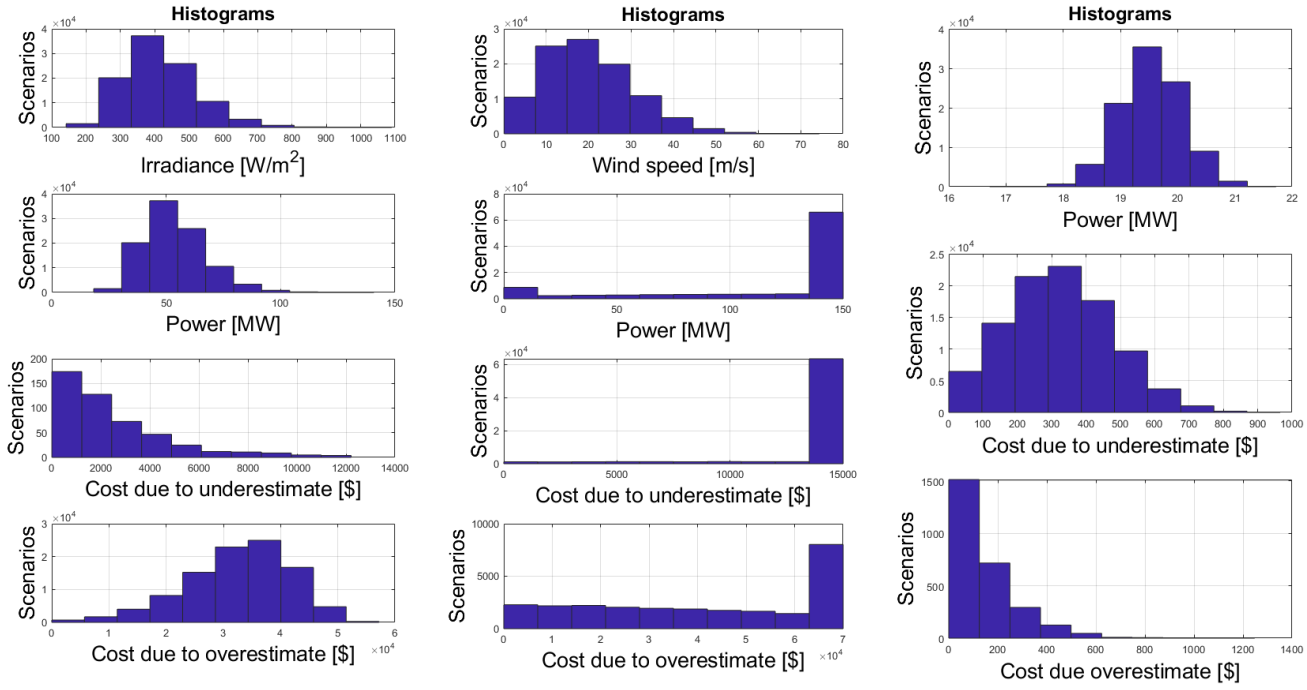

FIGURE 8. Histograms of the characteristics, power and costs associated to each renewable energy source.

the injected power is given by the power flow) and generator bus voltage set-points (54), 9 discrete variables related to stepwise adjustable on-load transformers' tap positions, 14 binary variables linked to switchable shunt compensation devices, and;

- 493 constraints for non-contingency conditions, and 492 constraints for each N-1 condition in each time instance (outages at branches 21, 50, 16 and 48). Constraints penalized in the fitness function: (i) Nodal voltages for load buses: 6 x (99 + 99); (ii) Allowable branch power flows: 6 x (186); (iii) Generator reactive power capability: 6 x (54 + 54), and (iv). Maximum active power output of a slack generator: 6 x (1).

Figure 8 shows one example of the Weibull probabilistic distribution [52] generated by Monte Carlo Simulation, meaning the calculated power for the randomly generates samples of renewable sources. It is important to note that the available power for each renewable is drawn according to its probability distribution that incurs in associated costs of underestimation and overestimation.

The uncertainty of power generation for the clean generators it also displayed. Regarding power available, we can see that the distribution of power in MW across the different scenarios is similar to a Gaussian distribution with mean value equal to 50 MW for PV and between 19 and 20 MW for electric vehicles. However, for WT the majority of the scenarios provide 150MW of power available. Due to the huge amount of wind power available, the cost due to underestimation is very high in most of the scenarios. On the other hand, the cost of underestimating solar power is concentrated in the smaller values, indicating that it is cheaper to store excess energy from PV.

For the electric vehicles the cost of underestimation is approximately normally distributed with mean at \$300/MW. With respect to the overestimation costs, as the electric vehicles generator contributes with a smaller power, its overestimation cost is small in most of the scenarios. As the power contribution to the grid increases, the cost due to overestimating power increases, as show in the PV costs. In the majority of the scenarios, WT power generated constitutes the major part of the power available in the grid, thus its cost of demanding more power than what is available is very high most of the simulated scenarios.

Considering renewable sources in this system, some thermal generators were replaced by solar, wind and vehicles. For the reliable and stable operation of an EV charging micro-grid system with a stochastic charging load, a robust coordinated controller is an essential requirement [10]. In this context we evaluated three techniques based on swarm intelligence properties, namely PSO, CE-EPSO and CE-CDEEPSO, who acted on the OARPD problem as a power grid controller system. Additionally, for each technique we also evaluated its modified version including the proposed local search operator.

Figure (9) illustrated the neighbor solutions obtained for one time instance for $d = 3$. It is important to note that although a solution considers all the six time instances, hence it lies in $\mathbb{R}^{780}$. We are illustrating the local search operation on

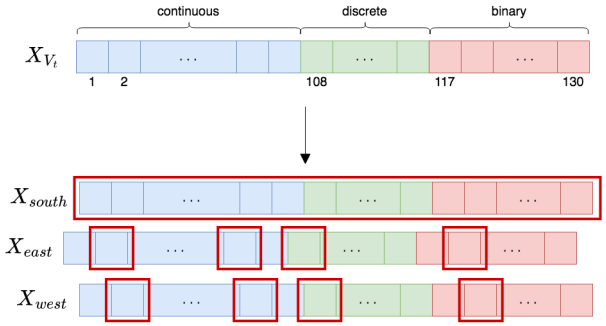

FIGURE 9. Illustration of the local search operator applied to solution vector in $\mathbb{R}^{130}$. In X_{south} all values are inverted. In X_{east} and X_{west}, only d values are modified plus one as previously showed by Algorithm 1.

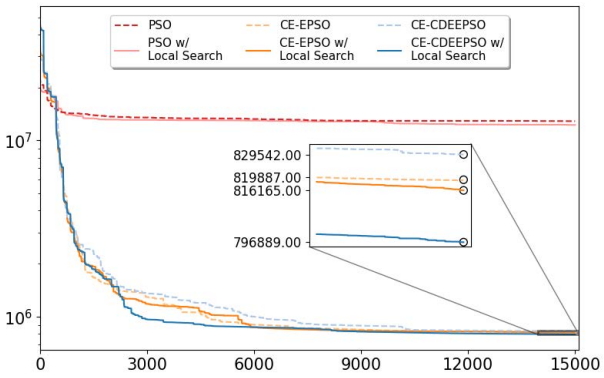

FIGURE 10. Convergence line of IEEE 118 bus system with electric vehicles and solar and wind generators.

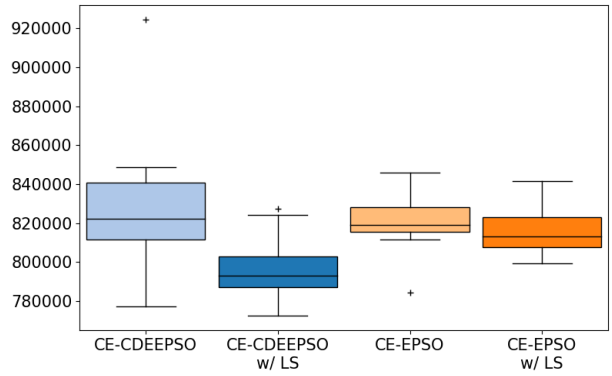

FIGURE 11. Boxplot results of IEEE 118 bus system with electric vehicles and solar and wind generators.

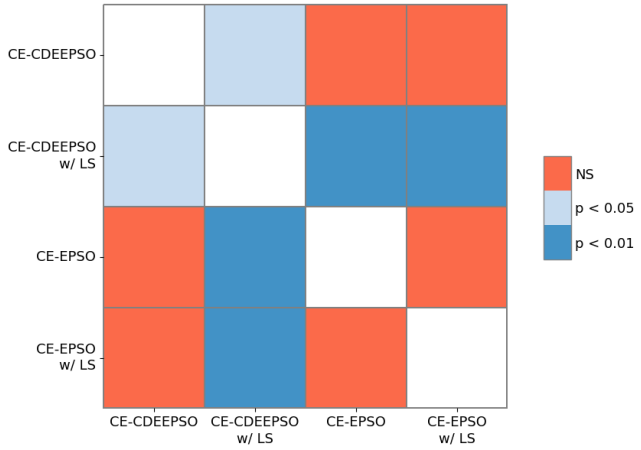

FIGURE 12. Heatmap of the p-values obtained after applying Connover test with Holm-Bonferroni correction to results of IEEE 118 bus system with electric vehicles and solar and wind generators. NS stands for non-significant.

only one time instance to facilitate understanding. However, the operation is carried in the solution vector composed by all the six time instances. Moreover, all the algorithms treat every variable as continuous. When inputting a solution to the test case system, discrete and binary variables are rounded to the closest integer value.

Due to the stochasticity of the solar, wind and vehicles generators, each algorithm was executed 10 times. Figure (10) shows the mean convergence line for each algorithm. Initially, it is possible to see that the standard PSO algorithm converged very early to a local minima and did not manage to escape from it. Even though the algorithm was trapped, the local search operator managed to converge to a lower cost. On the other hand, both CE-EPSO and CE-CDEEPSO showed a consistent decrease in the cost until iteration 12000. Furthermore, after 15000 iterations we can see that CE-EPSO was able to obtain a smaller average fitness than CE-CDEEPSO. Similarly to the outcome of employing the proposed local search operator in the standard PSO algorithm, the combination of the operator to CE-CDEEPSO and CE-EPSO achieved the smallest average fitness values. Moreover, the combination of CE-CDEEPSO with the proposed operator managed to achieve the smallest cost, saving $77104.00/day when compared to CE-EPSO with the local search.

Nevertheless, to provide a robust evaluation of the results obtained, we performed two non-parametric tests. Firstly we analyze the boxplot behaviour, then we conducted a pairwise comparison using Connover Test with Holm-Bonferroni correction. Figure (11) show the boxplots. We can see that the boxplot for CE-CDEEPSO with local search do not overlap any of the other. Hence, as stated in the previous subsection, we can affirm that there are differences from its mean to the other algorithms. However, it is not possible to attest whether there are differences between the using or not the local search operator in CE-EPSO. Thus, we performed pairwise corrections using a non-parametric statistical test entitled Connover Test along with Holm-Bonferroni correction to reduce the effect of multiple pairwise comparisons. Figure (12) shows a heat-map containing the p-values obtained for each comparison of algorithms.

At first we can see that, as attest from boxplot analysis, there are differences from CE-CDEEPSO with local search (LS) average fitness value to teh version with out LS, and both versions of CE-EPSO. Furthermore, the test shows that we

TABLE 5. Summary of the obtained results on each test case. A plus sign (+) indicates that there are statistical differences from the algorithm to the others with minus sign (−).

Metrics	Best ($/h)	Median ($/h)	Worst ($/h)	Mean ($/h)	Std. ($/h)
Case 1: IEEE 57-Bus System with Wind generators					
(+) CE-CDEEPSO	80379.81	80659.30	80949.57	80642.78	241.15
(-) CE-EPSO	85296.86	89882.94	117365.53	94954.90	10334.12
(-) PSO	96794.92	105563.41	201752.63	117977.34	31372.45
Case 2: IEEE 57-Bus System with Wind/Solar generators					
(+) CE-CDEEPSO	67186.45	67876.21	68178.53	67727.21	347.29
(-) CE-EPSO	70487.19	75083.86	89745.12	77211.40	6633.53
(-) PSO	92747.21	111436.35	141810.91	110281.18	16495.95
Case 3: IEEE 118-Bus System with Wind/Solar/EVs generators					
(+) CE-CDEEPSO w/ LS	772583.24	793191.45	827311.48	796891.53	17700.14
(-) CE-CDEEPSO	777221.63	822076.18	924404.59	829542.51	39380.09
(-) CE-EPSO w/ LS	799479.63	813215.51	841548.23	816164.13	12372.24
(-) CE-EPSO	784300.38	819285.38	845968.28	819887.99	16080.07
(-) PSO w/ LS	9263248.90	12255295.00	13598071.00	12252020.49	1183083.00
(-) PSO	11951245.00	12983657.50	13493854.00	12876826.10	542501.70

can attest that CE-CDEEPSO with LS differ from CE-EPSO (with and without LS) with 99% confidence. Another important information is that, although CE-EPSO (with LS) achieve a smaller average fitness value than its counterpart without local search, they are not statistically different. As a result, we can say that our algorithm CE-CDEEPSO combined to the proposed local search operator is suitable for the dynamic OPF problem, saving an average of 2.3 million dollars in a monthly average projection.

To summarize, Table 5 presents an overview of the obtained results for the two test cases evaluated under IEEE 57-Bus System and the third test case evaluated under IEEE 118-Bus System. As a validation of the mininum average fitness value obtained by CE-CDEEPSO in both IEEE 57-Bus System test cases, the plus sign (+) besides CE-CDEEPSO indicates that the mean fitness value is statistically different from the other mean fitness values with a minus sign (−). Moreover, CE-CDEEPSO standard deviation was more than 10 times smaller when compared to CE-EPSO and more than 20 times smaller when compared to PSO in both Case 1 and 2. This indicates that our algorithm managed to consistently achieve small fitness values throughout the different runs. Likewise, in the IEEE 118 Bus-System, the plus sign (+) indicates that CE-CDEEPSO with LS achieved the minimum average fitness value and it also statistically differ from the other algorithms. Regarding the local search operator, its combination to both CE-CDEEPSO and CE-EPSO led to not only smaller average fitness values but also a reduction in the standard deviation, providing more robust results.

V. CONCLUSION

In this work we have proposed an improvement of an evolutionary algorithm based on differential evolution (DE) and particle swarm optimization (PSO), entitled Canonical Differential Evolutionary Particle Swarm Optimization algorithm (C-DEEPSO). In the proposed modification we have included the cross-entropy (CE) method as a initial deep search to find a good basin of attraction for the initial population of C-DEEPSO. Then, we have also presented a novel local search operator that explores the neighborhood of each particle to try to find a better position.

This novel approach, known as CE-CDEEPSO, has been evaluated in solving the Optimal Active-Reactive Power Dispatch (OARPD) problem in microgrids, under two different test cases containing renewable energy sources. The first test case contained three wind turbines (WT) generators and the second test case contained two WT generators and one photovoltaic (PV) generator. The second test case was a bigger microgrid containing both WT and PV along with the addition of plugin electric vehicles (PEVs).

Results showed that CE-CDEEPSO outperformed alternative algorithms in IEEE 57 Bus-System test case (both scenarios), leading to a projected monthly saving average of 10 million dollars and 3.2 million dollars, respectively. Furthermore, in IEEE 118 Bus-system, CE-CDEEPSO with local search outperformed not only its counterpart without local search, but also the other algorithms considered. As a result, by using our proposal we were able to provide a projected monthly saving average of 2.3 million dollars in the microgrids systems considered. To conclude, both versions of CE-CDEEPSO proved to be suitable algorithms to solving OARPD problems involving wind turbines, photovoltaic panels and electric vehicles with a minimal cost and maintaining a reliable and stable operation. As future work lines, it would be important to evaluate our algorithm in even larger test cases, with an increased number of PV, WT generators and PEVs.

ACKNOWLEDGMENT

The authors thank UAH and UFRJ and for the infrastructure used to conduct this work, and Brazilian research agencies: CAPES (Finance Code 001) and CNPq for support.

REFERENCES

[1] M. J. Morshed, J. B. Hmida, and A. Fekih, "A probabilistic multi-objective approach for power flow optimization in hybrid wind-PV-PEV systems," *Appl. Energy*, vol. 211, pp. 1136–1149, Feb. 2018.

[2] S. P. Koko, "Optimal battery sizing for a grid-tied solar photovoltaic system supplying a residential load: A case study under south African solar irradiance," *Energy Rep.*, vol. 8, pp. 410–418, Aug. 2022.

[3] N. H. Awad, M. Z. Ali, R. Mallipeddi, and P. N. Suganthan, "An efficient differential evolution algorithm for stochastic OPF based active–reactive power dispatch problem considering renewable generators," *Appl. Soft Comput.*, vol. 76, pp. 445–458, Mar. 2019.
[4] D. Dabhi and K. Pandya, "Uncertain scenario based microgrid optimization via hybrid Levy particle swarm variable neighborhood search optimization (HL_PS_VNSO)," *IEEE Access*, vol. 8, pp. 108782–108797, 2020.
[5] C. Lamnatou, D. Chemisana, and C. Cristofari, "Smart grids and smart technologies in relation to photovoltaics, storage systems, buildings and the environment," *Renew. Energy*, vol. 185, pp. 1376–1391, Feb. 2022.
[6] M. A. Judge, A. Khan, A. Manzoor, and H. A. Khattak, "Overview of smart grid implementation: Frameworks, impact, performance and challenges," *J. Energy Storage*, vol. 49, May 2022, Art. no. 104056.
[7] O. B. Adewuyi, R. Shigenobu, K. Ooya, T. Senjyu, and A. M. Howlader, "Static voltage stability improvement with battery energy storage considering optimal control of active and reactive power injection," *Electric Power Syst. Res.*, vol. 172, pp. 303–312, Jul. 2019.
[8] T. Bunsen, P. Cazzola, M. Gorner, L. Paoli, S. Scheffer, R. Schuitmaker, J. Tattini, and J. Teter, "Global EV outlook 2018: Towards cross-modal electrification," Int. Energy Agency, 2018, p. 141, doi: 10.1787/9789264302365-en.
[9] M. T. Hussain, D. N. B. Sulaiman, M. S. Hussain, and M. Jabir, "Optimal management strategies to solve issues of grid having electric vehicles (EV): A review," *J. Energy Storage*, vol. 33, Jan. 2021, Art. no. 102114.
[10] Y. Wu, Z. Wang, Y. Huangfu, A. Ravey, D. Chrenko, and F. Gao, "Hierarchical operation of electric vehicle charging station in smart grid integration applications—An overview," *Int. J. Electr. Power Energy Syst.*, vol. 139, Jul. 2022, Art. no. 108005.
[11] Y. Wang, H. Liang, and V. Dinavahi, "Decentralized stochastic programming for optimal vehicle-to-grid operation in smart grid with renewable generation," *IET Renew. Power Gener.*, vol. 15, no. 4, pp. 746–757, Mar. 2021.
[12] M. Rahmani, S. H. Hosseinian, and M. Abedi, "Optimal integration of demand response programs and electric vehicles into the SCUC," *Sustain. Energy, Grids Netw.*, vol. 26, Jun. 2021, Art. no. 100414.
[13] F. Calise, F. L. Cappiello, M. D. D'Accadia, and M. Vicidomini, "Smart grid energy district based on the integration of electric vehicles and combined heat and power generation," *Energy Convers. Manage.*, vol. 234, Apr. 2021, Art. no. 113932.
[14] P. Aliasghari, B. Mohammadi-Ivatloo, and M. Abapour, "Risk-based scheduling strategy for electric vehicle aggregator using hybrid stochastic/IGDT approach," *J. Cleaner Prod.*, vol. 248, Mar. 2020, Art. no. 119270.
[15] W. Infante and J. Ma, "Coordinated management and ratio assessment of electric vehicle charging facilities," *IEEE Trans. Ind. Appl.*, vol. 56, no. 5, pp. 5955–5962, Sep. 2020.
[16] T. Nasir, S. Raza, M. Abrar, H. A. Muqeet, H. Jamil, F. Qayyum, O. Cheikhrouhou, F. Alassery, and H. Hamam, "Optimal scheduling of campus microgrid considering the electric vehicle integration in smart grid," *Sensors*, vol. 21, no. 21, p. 7133, Oct. 2021.
[17] M. Rekik and L. Krichen, "Photovoltaic and plug-in electric vehicle for smart grid power quality enhancement," *Arabian J. Sci. Eng.*, vol. 46, no. 2, pp. 1481–1497, Feb. 2021.
[18] A. Roudbari, A. Nateghi, B. Yousefi-khanghah, H. Asgharpour-Alamdari, and H. Zare, "Resilience-oriented operation of smart grids by rescheduling of energy resources and electric vehicles management during extreme weather condition," *Sustain. Energy, Grids Netw.*, vol. 28, Dec. 2021, Art. no. 100547.
[19] H. Dommel and W. Tinney, "Optimal power flow solutions," *IEEE Trans. Power App. Syst.*, vols. PAS–87, no. 10, pp. 1866–1876, Oct. 1968.
[20] C. G. Marcelino, J. V. C. Avancini, C. A. D. M. Delgado, E. F. Wanner, S. Jiménez-Fernández, and S. Salcedo-Sanz, "Dynamic electric dispatch for wind power plants: A new automatic controller system using evolutionary algorithms," *Sustainability*, vol. 13, no. 21, p. 11924, Oct. 2021.
[21] W. Liao, P. Li, Q. Wu, S. Huang, G. Wu, and F. Rong, "Distributed optimal active and reactive power control for wind farms based on ADMM," *Int. J. Electr. Power Energy Syst.*, vol. 129, Jul. 2021, Art. no. 106799.
[22] J. A. Momoh, R. Adapa, and M. E. El-Hawary, "A review of selected optimal power flow literature to 1993. I. Nonlinear and quadratic programming approaches," *IEEE Trans. Power Syst.*, vol. 14, no. 1, pp. 96–104, 1999.
[23] J. A. Momoh, M. E. El-Hawary, and R. Adapa, "A review of selected optimal power flow literature to 1993. II. Newton, linear programming and interior point methods," *IEEE Trans. Power Syst.*, vol. 14, no. 1, pp. 105–111, 1999.
[24] M. Papadimitrakis, N. Giamarelos, M. Stogiannos, E. N. Zois, N. A.-I. Livanos, and A. Alexandridis, "Metaheuristic search in smart grid: A review with emphasis on planning, scheduling and power flow optimization applications," *Renew. Sustain. Energy Rev.*, vol. 145, Jul. 2021, Art. no. 111072.
[25] Z. Xu, T. Deng, Z. Hu, Y. Song, and J. Wang, "Data-driven pricing strategy for demand-side resource aggregators," *IEEE Trans. Smart Grid*, vol. 9, no. 1, pp. 57–66, Jan. 2018.
[26] P. Rossoni, E. A. Belati, and R. D. S. Benedito, "A hybrid approach for optimization of electric power distributed networks with photovoltaic sources," *Electric Power Syst. Res.*, vol. 211, Oct. 2022, Art. no. 108183.
[27] P. P. Biswas, P. N. Suganthan, R. Mallipeddi, and G. A. J. Amaratunga, "Optimal reactive power dispatch with uncertainties in load demand and renewable energy sources adopting scenario-based approach," *Appl. Soft Comput.*, vol. 75, pp. 616–632, Feb. 2019.
[28] B. A. Kumari and K. Vaisakh, "Integration of solar and flexible resources into expected security cost with dynamic optimal power flow problem using a novel DE algorithm," *Renew. Energy Focus*, vol. 42, pp. 48–69, Sep. 2022.
[29] A. Askarzadeh, "A memory-based genetic algorithm for optimization of power generation in a microgrid," *IEEE Trans. Sustain. Energy*, vol. 9, no. 3, pp. 1081–1089, Jul. 2018.
[30] T. Praveen Kumar, N. Subrahmanyam, and S. Maheswarapu, "Genetic algorithm based power control strategies of a grid integrated hybrid distributed generation system," *Technol. Econ. Smart Grids Sustain. Energy*, vol. 6, no. 1, pp. 1–14, Dec. 2021.
[31] Z. Ullah, S. Wang, J. Radosavljevic, and J. Lai, "A solution to the optimal power flow problem considering WT and PV generation," *IEEE Access*, vol. 7, pp. 46763–46772, 2019.
[32] E. Rashedi, H. Nezamabadi-pour, and S. Saryazdi, "GSA: A gravitational search algorithm," *Inf. Sci.*, vol. 179, no. 13, pp. 2232–2248, Jun. 2009.
[33] R. Jamal, B. Men, N. H. Khan, M. A. Z. Raja, and Y. Muhammad, "Application of Shannon entropy implementation into a novel fractional particle swarm optimization gravitational search algorithm (FPSOGSA) for optimal reactive power dispatch problem," *IEEE Access*, vol. 9, pp. 2715–2733, 2021.
[34] L. Kumar, M. K. Kar, and S. Kumar, "Statistical analysis based reactive power optimization using improved differential evolutionary algorithm," *Exp. Syst.*, Jun. 2022, Art. no. e13091.
[35] Y. Wang, A. O. Rousis, and G. Strbac, "Resilience-driven optimal sizing and pre-positioning of mobile energy storage systems in decentralized networked microgrids," *Appl. Energy*, vol. 305, Jan. 2022, Art. no. 117921.
[36] F. García-Muñoz, F. Díaz-González, and C. Corchero, "A novel algorithm based on the combination of AC-OPF and GA for the optimal sizing and location of DERs into distribution networks," *Sustain. Energy, Grids Netw.*, vol. 27, Sep. 2021, Art. no. 100497.
[37] M. Niu, N. Z. Xu, H. N. Dong, Y. Y. Ge, Y. T. Liu, and H. T. Ngin, "Adaptive range composite differential evolution for fast optimal reactive power dispatch," *IEEE Access*, vol. 9, pp. 20117–20126, 2021.
[38] B. A. Kumari and K. Vaisakh, "Ensuring expected security cost with flexible resources using modified DE algorithm based dynamic optimal power flow," *Appl. Soft Comput.*, vol. 124, Jul. 2022, Art. no. 108991.
[39] R. Y. Rubinstein, "Optimization of computer simulation models with rare events," *Eur. J. Oper. Res.*, vol. 99, no. 1, pp. 89–112, 1997.
[40] P. P. Biswas, P. N. Suganthan, R. Mallipeddi, and G. A. J. Amaratunga, "Optimal power flow solutions using differential evolution algorithm integrated with effective constraint handling techniques," *Eng. Appl. Artif. Intell.*, vol. 68, pp. 81–100, Feb. 2018.
[41] C. G. Marcelino, P. E. M. Almeida, E. F. Wanner, M. Baumann, M. Weil, L. M. Carvalho, and V. Miranda, "Solving security constrained optimal power flow problems: A hybrid evolutionary approach," *Appl. Intell.*, vol. 48, no. 10, pp. 3672–3690, Oct. 2018.
[42] H. Bouchekara, "Solution of the optimal power flow problem considering security constraints using an improved chaotic electromagnetic field optimization algorithm," *Neural Comput. Appl.*, vol. 32, no. 7, pp. 2683–2703, Apr. 2020.
[43] J. Zhu, X. Mo, Y. Xia, Y. Guo, J. Chen, and M. Liu, "Fully-decentralized optimal power flow of multi-area power systems based on parallel dual dynamic programming," *IEEE Trans. Power Syst.*, vol. 37, no. 2, pp. 927–941, Mar. 2022.
[44] S. Rivera, A. Al-Sumaiti, D. Rodriguez, M. Gers, J. Rueda, K. Lee, and I. Erlich, "Emerging heuristic optimization algorithms for operational planning of sustainable electrical power systems," *IEEE PES Competition. Tech. Report.*, vol. 1, pp. 1–13, 2018.

[45] J. C. Arevalo, F. Santos, and S. Rivera, "Uncertainty cost functions for solar photovoltaic generation, wind energy generation, and plug-in electric vehicles: Mathematical expected value and verification by Monte Carlo simulation," *Int. J. Power Energy Convers.*, vol. 10, no. 2, pp. 171–207, Jan. 2019.
[46] J. Kennedy and R. Eberhart, "Particle swarm optimization," in *Proc. IEEE ICNN*, vol. 4. Nov./Dec. 1995, pp. 1942–1948.
[47] C. G. Marcelino, G. M. C. Leite, C. A. D. M. Delgado, L. B. de Oliveira, E. F. Wanner, S. Jiménez-Fernández, and S. Salcedo-Sanz, "An efficient multi-objective evolutionary approach for solving the operation of multi-reservoir system scheduling in hydro-power plants," *Exp. Syst. Appl.*, vol. 185, Dec. 2021, Art. no. 115638.
[48] C. Marcelino, M. Baumann, L. Carvalho, N. Chibeles-Martins, M. Weil, P. Almeida, and E. Wanner, "A combined optimisation and decision-making approach for battery-supported HMGS," *J. Oper. Res. Soc.*, vol. 71, no. 5, pp. 762–774, May 2020.
[49] P. Boer, D. Kroese, S. Mannor, and R. Rubinstein, "A tutorial on the cross-entropy method," *Ann. Oper. Res.*, vol. 134, pp. 19–67, Jan. 2005.
[50] L. de Magalhaes Carvalho, A. M. Leite da Silva, and V. Miranda, "Security-constrained optimal power flow via cross-entropy method," *IEEE Trans. Power Syst.*, vol. 33, no. 6, pp. 6621–6629, Nov. 2018.
[51] C. G. Marcelino, C. Camacho-Gómez, S. Jiménez-Fernández, and S. Salcedo-Sanz, "Optimal generation scheduling in hydro-power plants with the coral reefs optimization algorithm," *Energies*, vol. 14, no. 9, p. 2443, Apr. 2021.
[52] T. Arslan, Y. M. Bulut, and A. A. Yavuz, "Comparative study of numerical methods for determining Weibull parameters for wind energy potential," *Renew. Sustain. Energy Rev.*, vol. 40, pp. 820–825, Dec. 2014.

CAROLINA GIL MARCELINO was born in Belo Horizonte, Brazil, in 1984. She received the Ph.D. degree in mathematical and computing modeling from the Centro Federal de Educação Tecnológica de Minas Gerais, Brazil, in 2017. She spent two years with the Department of Signal Processing and Communications, Universidad de Alcalá, Spain, as a Postdoctoral MSCA Researcher, cofunded by the H2020 in the GOT Energy Talent Program. She is currently an Adjunct Professor at the Computing Institute, Universidade Federal do Rio de Janeiro, Brazil, where she carries out research on population-based optimization, multi-criteria decision-aid, and machine learning for applications in energy domain.

GABRIEL MATOS CARDOSO LEITE was born in Rio de Janeiro, Brazil, in 1992. He received the B.S. and M.Sc. degrees in computer science and systems engineering and computer science from the Universidade Federal do Rio de Janeiro, Brazil, in 2017 and 2019, respectively, where he is currently pursuing the Ph.D. degree in systems engineering and computer science program, with a focus on mobility on Universidad de Alcalá, Spain, where he carries out research on optimization and machine learning techniques.

SILVIA JIMÉNEZ-FERNÁNDEZ was born in Madrid, Spain, in 1976. She received the B.S. and Ph.D. degrees in telecommunications engineering from the Universidad Politécnica de Madrid, Spain, in 1999 and 2009, respectively. She is currently an Associate Professor with the Department of Signal Processing and Communications, Universidad de Alcalá, Madrid, where she carries out research on the application of signal processing and machine learning techniques for mobile communication systems.

SANCHO SALCEDO-SANZ was born in Madrid, Spain, in 1974. He received the B.S. degree in physics from the Universidad Complutense de Madrid, Spain, in 1998, the Ph.D. degree in telecommunications engineering from the Universidad Carlos III de Madrid, Spain, in 2002, and the Ph.D. degree in physics from the Universidad Complutense de Madrid, in 2019. He spent one year with the School of Computer Science, University of Birmingham, U.K., as a Postdoctoral Research Fellow. He is currently a Full Professor with the Department of Signal Processing and Communications, Universidad de Alcalá, Spain. He has coauthored more than 230 international journal articles in the field of machine learning and soft-computing. His current research interests include deal with soft-computing techniques, hybrid algorithms, and neural networks in different applications of science and technology.